Available online at www.sciencedirect.com
ScienceDirect
Tetrahedron: Asymmetry
Tetrahedron: *Asymmetry* 17 (2006) 3430–3436

Synthesis, resolution, and absolute configuration of two novel and selective cyclooxygenase-2 inhibitors based on the 1,5-diarylpyrrole structure

Lorenzo Di Bari,[a] Gennaro Pescitelli,[a] Piero Salvadori,[a,*] Michele Rovini,[b] Maurizio Anzini,[b,*] Andrea Cappelli[b] and Salvatore Vomero[b]

[a]*Dipartimento di Chimica e Chimica Industriale, Università di Pisa, Via Risorgimento 35, 56126 Pisa, Italy*
[b]*Dipartimento Farmaco Chimico Tecnologico and European Research Centre for Drug Discovery and Development, Università di Siena, Via A. Moro, 53100 Siena, Italy*

Received 30 November 2006; accepted 19 December 2006

Abstract—Three racemic esters based on the 1,5-diarylpyrrole structure, which proved to be highly selective COX-2 inhibitors endowed with an appreciable anti-inflammatory activity in some animal models, were subjected to chiral resolution. Their absolute configurations were assigned by comparison of the CD spectrum measured on-line with a HPLC–CD detector, with that calculated by means of a TDDFT method.

1. Introduction

Commercially available nonsteroidal anti-inflammatory drugs (NSAIDs) (e.g., aspirin, indometacin, and diclofenac) are generally effective and widely used for the treatment of inflammatory conditions.[1–3] However, the disruption of beneficial prostaglandin (PG) production by all the currently used NSAIDs results in a mechanism-based toxicity mainly in the gastrointestinal (GI) tract and in the kidney,[4–6] thus limiting their therapeutic usefulness, especially when long-term treatment is involved.

More than a decade ago, an inducible cyclooxygenase (COX) isozyme, now commonly known as COX-2, was discovered and found to be expressed primarily in inflamed tissues.[7–10]

As a result, substantial effort has been undertaken in the pharmaceutical industry to identify selective and orally active COX-2 inhibitors[11,12] able to provide the desired anti-inflammatory and analgesic profiles, without the deleterious side effects commonly associated with the existing NSAIDs.

Several distinct classes of selective COX-2 inhibitors have been reported in the literature.[13] Most of these selective COX-2 inhibitors belong to the diaryl heterocyclic class, also known as the 'coxibs', and have demonstrated potent anti-inflammatory activity in the rat adjuvant-induced arthritis model along with exceptional safety profiles in comparison with the current NSAIDs. Amongst these compounds, celecoxib[14] (SC58635, Celebrex®, **1**) and rofecoxib[15] (MK-966, Vioxx®, **2**) constitute the most representative and widely marketed drugs (Chart 1).

As part of our research program aimed at discovering new pyrrole-containing anti-inflammatory agents, we have successfully identified a novel series of 1,5-diarylpyrrole-3-acetic acids and esters **3** as new, potent, and selective COX-2 inhibitors,[16] in which the pyrroleacetic and vicinal diaryl heterocyclic moieties are reminiscent both of indometacin **4** and of the above-cited 'coxib' family, respectively.

In order to increase our knowledge on the COX-2 inhibitory activity of 1,5-diarypyrroles functionalized at the 3-position of the pyrrole moiety, we synthesized racemic

* Corresponding authors. Tel.: +39 050 2219203; fax: +39 050 2219409 (P.S.); tel.: +39 0577 234173; fax: +39 0577 234333 (M.A.); e-mail addresses: psalva@dcci.unipi.it; anzini@unisi.it

0957-4166/$ - see front matter © 2007 Elsevier Ltd. All rights reserved.
doi:10.1016/j.tetasy.2006.12.019

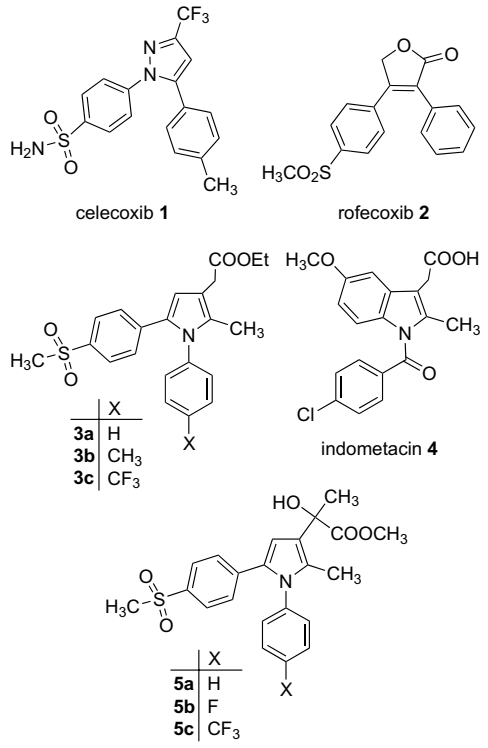

Chart 1.

esters **5**, resolved them by HPLC and assigned their absolute configuration.

Efficient racemate separation conditions could be found for compounds **5a** and **5b**, and their CD spectra measured on-line using a HPLC–CD detector.[17] The absolute configurations were then assigned by comparison with CD spectra[18] computed using the TDDFT method.[19] The input structures were obtained by DFT geometry optimizations following a thorough conformational study with computational (DFT, AM1) and spectroscopic techniques (^{1}H NOESY, variable temperature NMR).

2. Results and discussion

2.1. Synthesis of compounds 5a–c

The synthesis of racemic esters **5**, as shown in Scheme 1, was accomplished starting from the suitable 3-unsubstituted 1,5-diarylpyrrole **6** prepared, as previously reported,[16] via a regioselective acylation with methyl pyruvate in the presence of $TiCl_4$ to give the expected derivatives **5** in satisfactory yield. In order to assign the absolute configuration of compounds **5a–c**, we first considered the possibility of acylating the hydroxyl group to obtain suitable bi-chromophoric derivatives for application of the exciton chirality method.[20] The pre-existing 2-arylpyrrole chromophore absorbs in the 300–350 nm region ($\varepsilon_{max} = 16{,}700$ at $\lambda_{max} = 329$ nm for **5a** in acetonitrile); therefore, we looked at 4-methoxy cinnamate ($\lambda_{max} = 310$ nm) as the most appropriate candidate for an efficient exciton coupling.[20] Unfortunately, in the present case, various reported derivatization procedures[21] were unsuccessful, probably due to the high steric hindrance caused by the different substituents at the asymmetric carbon, which made the tertiary alcohol completely unreactive. In order to overcome this obstacle, we resolved to proceed directly to the chiral separation of racemic esters **5a–c** by means of enantioselective HPLC.

2.2. Enantioselective HPLC of compounds 5a and 5b

In order to obtain a fast, direct method for the resolution of racemates **5a–c**, we attempted several procedures of chiral liquid chromatography. Preliminary baseline separation of **5a** was successfully performed by HPLC with an amylose carbamate CSP (Chiralcel AD®), on an analytical scale of the racemate, by first eluting with an *i*-PrOH/*n*-hexane (70:30 v/v) mixture at a flow rate of 0.30 mL/min; in a second attempt to improve the enantioselectivity of the column, the amount of *i*-PrOH was lowered from 70% to 60%. Under these conditions, the enantiomers of compound **5a** were separated showing a retention time of 16.7 and 18.4 min, respectively.

Unfortunately, the chiral separation of racemate of **5c** was unsuccessful, while the racemates of compounds **5a** and **5b** were definitively separated by enantioselective HPLC with CD detection on-line, under the above-cited conditions. Figure 1a displays the elution profile obtained for **5a** upon setting the detection wavelength (for both the absorption and the CD detectors) to 330 nm, corresponding to the absorption maximum observed in the UV spectrum measured on a racemic sample of **5a**. The first eluted enantiomers of **5a** and **5b** showed a positive CD signal at 330 nm, while the second eluted ones showed a negative CD (Fig. 1a; data for **5b** not shown). The CD spectra measured on-line,[17] in correspondence with the two elution peaks of **5a**, are almost perfect mirror-images (Fig. 1b); the anisotropy *g*-value $\Delta A/A$ for the most intense CD

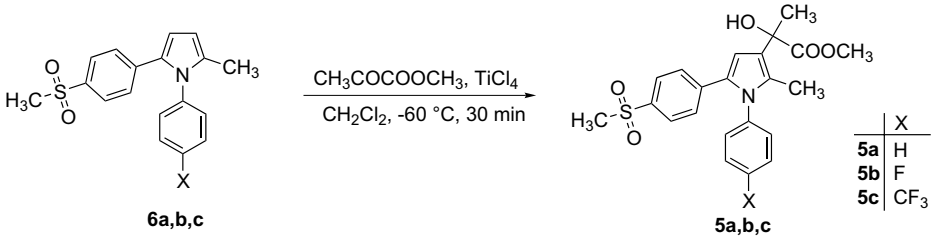

Scheme 1.

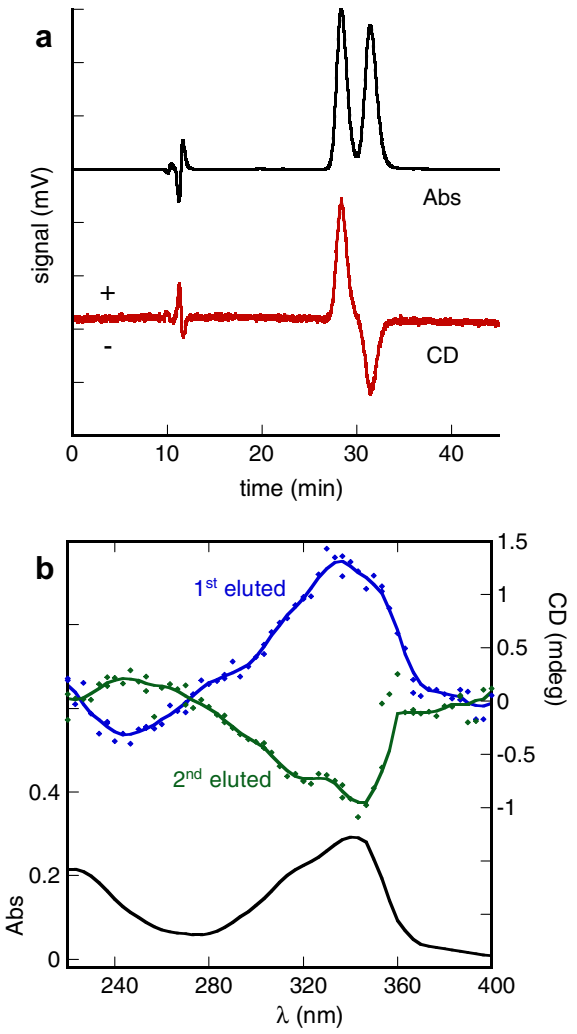

Figure 1. (a) Chromatogram of the enantioselective separation of **5a**. Conditions: Chiralpak® AD column, eluent hexane/2-propanol 60:40, flux 0.3 mL/min, detector (Abs and CD) wavelength 330 nm. (b) CD and absorption spectra measured on-line in correspondence with elution peaks.

signal of compounds **5a**–**b** is of the order of 10^{-4}, intense enough to obtain an acceptable CD signal-to-noise ratio. The first eluted enantiomer of **5a** displays a broad positive CD band at 280–370 nm, with the maximum at 335 nm and a shoulder on the short wavelength side (more clearly seen for the second eluted compound), plus a negative peak centered around 245 nm.

2.3. Conformational study of compound 5a

The knowledge of the solution conformation is a fundamental prerequisite for interpreting the CD spectra for the determination of absolute configuration. In what follows, we focus on compound **5a**; our results can easily be extended to **5b**. Upon inspection of the molecular structure, several degrees of freedom may be expected to concur to the overall conformation adopted by **5a** (see bold bonds in Chart 2): the C3–C2′, the C2′–OH, and C1′–C2′ torsions in the proximity of the chiral center; the N1-phenyl and the

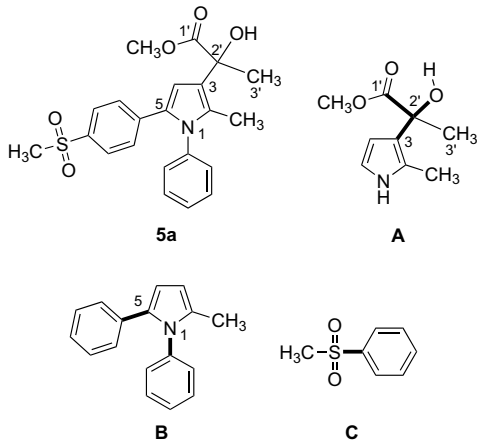

Chart 2.

C5-aryl torsions on the opposite side of the molecule; and finally, the aryl-S(=O) torsion. The problem may be simplified by taking into account the three sets of torsions independently of each other, which ends up in examining the three model compounds **A**, **B**, and **C**.

The ^{1}H NMR spectrum of **5a** in $CDCl_3$ or CD_3CN consists of a single set of peaks. Selective 1D-NOESY spectra showed, among others, a diagnostic NOE correlation between H4 and C3′ methyl protons, with comparable intensity in the two solvents employed; no Overhauser enhancement was detected between the C2-attached and C3′ methyls (Scheme 2). The chemical shift for the hydroxyl proton varied somewhat downfield upon heating the sample, moving from 3.663 ppm at 280 K to 3.518 ppm at 323 K in $CDCl_3$, and from 4.105 to 3.887 ppm in CD_3CN. A linear δ (ppm) vs. T (K) relationship was observed (linear correlation $R > 0.9998$) with a slope $\Delta\delta_{OH}/\Delta T = 3.4$ ppb/deg in $CDCl_3$. Such a relatively small value for the temperature coefficient indicates a reduced mobility of the hydroxyl proton consistent with an intramolecular hydrogen bond; the commonly accepted threshold for diagnosing an intramolecular hydrogen bond is in fact 4.6 ppb/deg.[22] In CD_3CN, a solvent with stronger hydrogen bond acceptor capacity, which would mimic the eluent mixture used for HPLC,[23] the temperature coefficient amounts to $\Delta\delta_{OH}/\Delta T = 5.0$ ppb/deg ($R > 0.9997$), only slightly above the threshold. Interestingly, the hydrogen bond is preserved in the solid state: the IR stretching frequency for the ester bond was observed at 1728 cm^{-1} (KBr disk), a value expected for ester groups involved as hydrogen bond acceptors.[24] In conclusion in the case of **5a**, the experimental data support the structure sketched in Scheme 2.

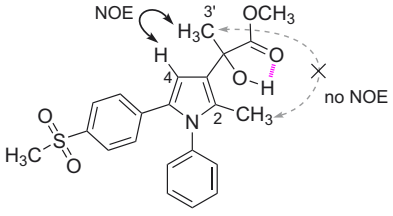

Scheme 2.

Molecular modelling of compound **A** started with a double torsional AM1 energy scan relative to C3–C2′ and C1′–C2′ torsions varied each in the 0–360° range by 15° steps. This resulted in 4 low-energy regions within which 8 structures were found as local AM1-energy minima. They were then optimized with B3LYP/6-31G(d) and converged in 4 final structures. Two of them, the lowest energy one and the second most stable (+0.034 kcal/mol), showed an arrangement (Fig. 2) clearly compatible with the experimental data: in particular, the C3′–C2′–C3–C4 dihedral attains such values able to justify the NOESY results, while the C2′–OH and C1′–C2′ torsions allow for the intramolecular hydrogen bond. No experimental definite proof was found for the two remaining DFT structures with much higher energy (over +1.30 kcal/mol above the absolute minimum); they were therefore discarded.

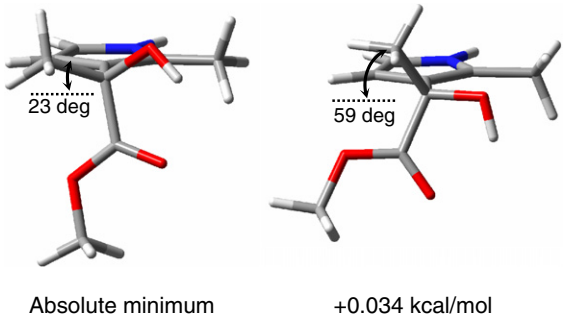

Figure 2. The two lowest energy conformers (and relative C3′–C2′–C3–C4 dihedral values) computed by B3LYP/6-31G(d) for model **A**.

The two aryl–aryl torsions relevant for model **B** are clearly correlated and will depend on a balance of conjugative and steric effects (also involving C2-methyl). DFT geometry optimizations with B3LYP/6-31G(d) showed two enantiomorphic structures where N1-phenyl and C5-phenyl dihedrals were found to be equal to −58/−37° and +58/+37°. Finally, for methyl phenyl sulfone (**C**) a single minimum is obtained with B3LYP/6-31G(d) with S–CH_3 bond perpendicular to the aromatic plane.

On the basis of the above-mentioned results, four structures were constructed and optimized with B3LYP/6-31G(d) and the four final geometries **I-p**, **II-p**, **I-n**, and **II-n** were obtained; they are shown in Figure 3 with their relative energies and Boltzmann population at 300 K (roman numbers refer to the arrangement of the C3 substituent, and n/p to the sign of aryl–aryl dihedrals). It is clear that as all the four geometries may give a sizeable contribution to the CD spectrum, they all need to be considered in what follows; for each geometry, a structural analogue with the opposite orientation for the sulfone group should be considered too, but this has small influence on the calculated CD (vide infra).

2.4. CD calculation on compound 5a and configurational assignment

Figure 4a shows CD spectra computed for the four geometries **I-n**, **II-n**, **I-p**, and **II-p** with (*S*)-configuration, and their Boltzmann-weighted average at 300 K. The main parameter determining the CD shape is evidently the couple of aryl–aryl dihedrals. The fact that **I-n** and **II-n** have much more intense CD spectra in the long wavelength region than **I-p** and **II-p** is reassuring because a reasonable variation in the population of the various conformers (which may only be predicted by calculations but not checked experimentally) would not lead to a sign reversal for the diagnostic bands in the average spectrum. Moreover, the similarity between the spectra computed for **I-n** and **II-n** indicates that the conformation adopted by the C3-attached chain is not crucial.[†]

Figure 4b shows computed rotational strengths for **I-n**, which represents the major contributor to the average spectrum. From the analysis of computed transitions and Kohn-Sham orbitals, it can be concluded that the first and most intense CD band is due to a π–π* type HOMO–LUMO transition (#1 in Fig. 4b); it mainly involves π orbitals belonging to the pyrrole and to the C5-attached aryl ring, which are mixed to some extent with σ and n-type orbitals localized on the substituent at C3. The second apparent CD band results from the overlap between four transitions (#5 to #8 in Fig. 4b) assigned as follows: #5, charge-transfer type transition from N1-attached aryl π to the LUMO π*; #6, HOMO π to ester π* transition; #7 and #8, further aromatic π–π* transitions localized on the three rings. Incidentally, a 180° flip of the sulfone group in **I-n** had only minor consequences on the computed CD spectrum. It is also worth saying that the eight transitions contributing to the CD above 240 nm have energies well below the estimated ionization potential (5.74 eV) and involve Kohn-Sham orbitals with negative eigenvalues, two conditions which increase the accuracy of TDDFT calculations.[19]

The position and relative intensity of the two visible bands in the average computed spectrum (Fig. 4a, thick black line) are in good agreement with the experimental CD (Fig. 1b). The CD sign predicted for (*S*)-absolute configuration is positive at longer wavelengths and negative at shorter wavelengths; therefore, the first eluted enantiomer for **5a** (positive CD at 330 nm) may be assigned the (*S*)-absolute configuration. Similarly, the first eluted enantiomer for **5b** (positive CD at 330 nm) may be assigned the (*S*)-absolute configuration, based on the consistency of its spectral and conformational data (not shown) with those of **5a**. Finally, given the remote *para*-position of the N1-attached aromatic substituents with respect to the reaction site at C3 for the synthesis of products **5** (Scheme 1), we may infer the same (*S*)-[CD (+) at 330 nm] configuration for **5c**.

[†] A structure with no intramolecular hydrogen bond, generated from **I-n** upon a 180° flip of both C2′–O and C1′–C2′ torsions followed by geometry optimization with B3LYP/6-31G(d), showed a TDDFT calculated CD spectrum similar to that of **I-n**, except for a higher intensity in the short wavelength region (due to a fourfold more intense computed rotational strength for transition #6, while other bands had comparable strengths). This structure was the one with the lowest energy available with no hydrogen bond and compatible with the NOESY data in CD_3CN.

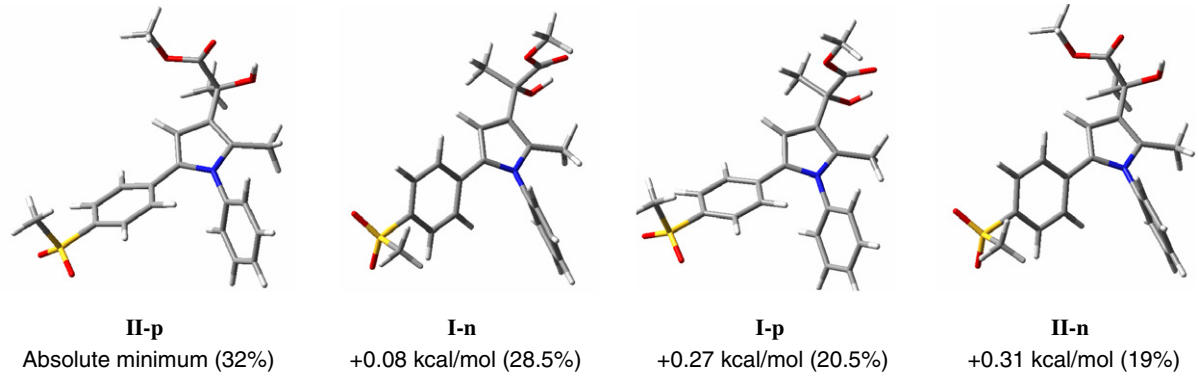

Figure 3. Structures, relative energies and Boltzmann populations at 300 K for the lowest energy conformers computed by B3LYP/6-31G(d) for compound **5a**.

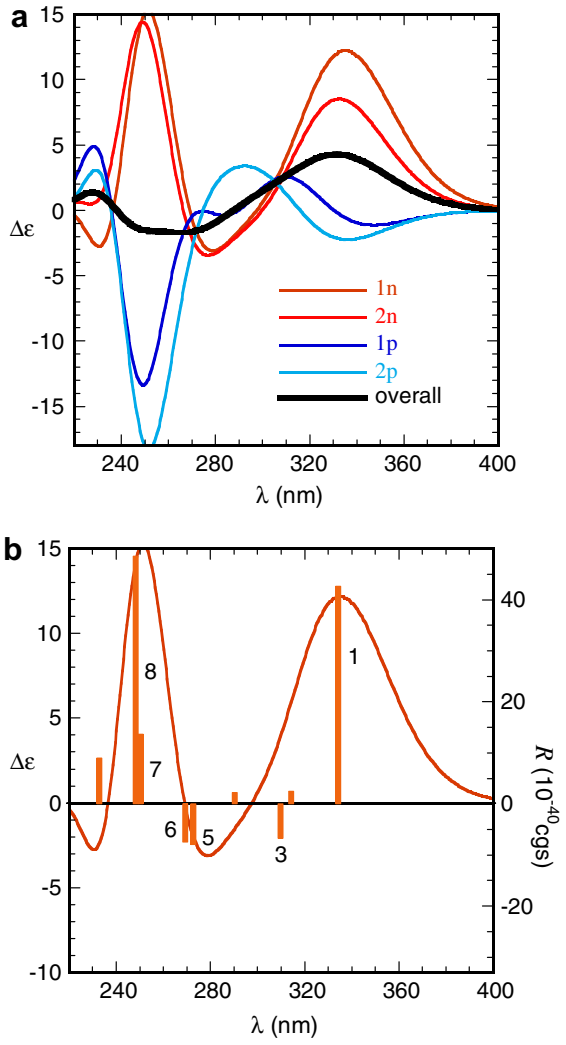

Figure 4. (a) TDDFT-computed CD spectra with B3LYP/TZVP for the four lowest energy conformers of **5a** and average spectrum calculated as Boltzmann-weighted average at 300 K. (b) Spectrum computed for structure **I-n** showing calculated rotational strengths *R* as vertical bars.

3. Conclusions

The absolute configuration of novel COX-2 inhibitors **5** has been assigned as (*S*)-[CD (+) at 330] based on the comparison between TDDFT calculations and CD measured on-line during enantioselective HPLC separation. The present assignment represents the first step toward investigation of the impact of absolute stereochemistry on the activity and selectivity of 1,5-diarylpyrrole-based COX-2 inhibitors.[25] In fact, the second step will be the isolation of the enantiomers originating from a semipreparative chromatographic procedure, in order to recover them in sufficient quantities to make biological evaluation feasible so as to assess the possible influence of chirality on the pharmacological properties of this class of compounds.

4. Experimental

4.1. Chemistry and equipments

All chemicals used were of reagent grade. Yields refer to purified products and are not optimized. Melting points were determined in open capillaries on a Gallenkamp apparatus and are uncorrected. Merck silica gel 60 (230–400 mesh) was used for column chromatography. Merck TLC plates and silica gel 60 F_{254} were used for TLC. ^{1}H NMR spectra were recorded with a Bruker AC 200 spectrometer in the indicated solvent (TMS as internal standard). The values of the chemical shifts are expressed in ppm, and the coupling constants (*J*) are expressed in Hz. Additional NMR spectra were recorded with a Varian INOVA 600 spectrometer operating at 14.1 T. In the 1D-NOESY experiments, protons C2–CH_3, C4–H, and 3′-CH_3 were selectively inverted with sech pulses; duration and B1 values (in ms and Hz) were 35.9/105, 11.3/332, and 42.8/93.7, respectively. Mass spectra were recorded on either a Varian Saturn 3 or a ThermoFinningan LCQ-deca spectrometer. IR spectra were recorded as KBr discs with a Perkin Elmer 1600 FTIR. Enantioselective HPLC separations were executed on a Daicel Chiralpak AD column using a Jasco PU-887 pump equipped with a Jasco CD-1595 detector, under the following conditions: eluent hexane/2-propanol 60:40 (for **5a**) or 70:30 (**5b**); flow 0.3 mL/min, detector (UV and CD) wavelength 330 nm. CD spectra were measured on-line with the CD detector during the HPLC separations, as the average of three different scans acquired in correspondence with each elution peak (wave-

length range 220–420 nm, total acquisition time 1 min, time resolution 0.6 s).

4.2. General procedure for the preparation of 5a–c

To a solution of the suitable pyrrole derivative **6a–c** (0.72 mmol) and methyl pyruvate (1.08 mmol) in dry CH_2Cl_2 (15 mL), $TiCl_4$ (0.72 mmol) was slowly added at −60 °C under an argon atmosphere. The mixture was stirred at −60 °C for an additional 30 min and after this time, when the temperature rose to 25 °C, was poured onto crushed ice and extracted with CH_2Cl_2. The organic phase was washed with brine, dried, and evaporated under reduced pressure. The residue, purified by flash-chromatography (EtOAc/hexane 6:4 v/v), afforded the required product.

4.3. Methyl 2-hydroxy-2-[2-methyl-5-(4-(methylsulfonyl)-phenyl)-1-phenyl-1*H*-pyrrol-3-yl]propanoate 5a

White needles from ethyl acetate, mp 142–144 °C (yield 80%). ^{1}H NMR ($CDCl_3$) δ ppm: 1.83 (s, 3H), 2.10 (s, 3H), 2.96 (s, 3H), 3.60 (br s, 1H), 3.80 (s, 3H), 6.54 (s, 1H), 7.13 (m, 4H), 7.37 (m, 3H), 7.62 (m, 2H). MS-ESI: m/z 436 ($M+Na^+$).

4.4. Methyl 2[1-(4-fluorophenyl)-2-methyl-5-(4-(methyl-sulfonyl)phenyl)-1*H*-pyrrol-3-yl]-2-hydroxypropanoate 5b

White needles from ethyl acetate, mp 177–179 °C (yield 95%). ^{1}H NMR ($CDCl_3$) δ ppm: 1.84 (s, 3H), 2.10 (s, 3H), 2.98 (s, 3H), 3.58 (br s, 1H), 3.82 (s, 3H), 6.54 (s, 1H), 7.08–7.17 (m, 6H), 7.68 (m, 2H). MS-ESI: m/z 454 ($M+Na^+$).

4.5. Methyl 2-[2-methyl-5-(4-(methylsulfonyl)phenyl)-1-(4-(trifluoromethyl)phenyl)-1*H*-pyrrol-3-yl]-2-hydroxypropanoate 5c

White needles from ethyl acetate, mp 144–146 °C (yield 70%). ^{1}H NMR ($CDCl_3$) δ ppm: 1.80 (s, 3H), 2.10 (s, 3H), 2.96 (s, 3H), 3.62 (br s, 1H), 3.78 (s, 3H), 7.08 (s, 1H), 7.10 (m, 2H), 7.24 (m, 2H), 7.64 (m, 4H). MS-ESI: m/z 504 ($M+Na^+$).

5. Computational

All computations were performed using Gaussian'03.[26] Geometry scans and optimizations were executed with semi-empirical method AM1 and the DFT method employing the B3LYP hybrid functional and 6-31G(d) basis set.[27] Excited states calculations were executed with TDDFT method employing the B3LYP functional and the triple-ζ split valence basis TZVP.[27] CD spectra were generated from Gaussian'03 outputs using dipole length-computed rotational strengths (dipole-velocity values differed by less than 10% for the main transitions), to which a Gaussian band-shape was applied with 4170 cm^{-1} half-height width (corresponding to 45 nm at 330 nm).

Acknowledgments

M.A. wishes to thank Dr. Antonio Giordani (Rottapharm SpA, Monza, Italy) for partial financial support. Professor Stefania D'Agata D'Ottavi's careful reading of the manuscript is also acknowledged.

References

1. Vane, J. R. *Nature (London) New Biol.* **1971**, *231*, 232–235.
2. Smith, J. B.; Willis, A. L. *Nature (London) New Biol.* **1971**, *231*, 235–237.
3. Lombardino, J. G. *Nonsteroidal Antiinflammatory Drugs*, 1st ed.; John Wiley & Son: New York, 1985.
4. Allison, M. C.; Howatson, A. G.; Torrance, C. J.; Lee, F. D.; Russell, R. I. G. *N. Eng. J. Med.* **1992**, *327*, 749–754.
5. Clive, D. M.; Stoff, J. S. *N. Eng. J. Med.* **1984**, *310*, 563–572.
6. Pirson, Y.; Van Ypersele de Strihou, C. *Am. J. Kidney Dis.* **1986**, *8*, 337–344.
7. Hla, T.; Neilson, K. *Proc. Natl. Acad. Sci. U.S.A.* **1992**, *89*, 7384–7388.
8. Xie, W.; Chipman, J. G.; Robertson, D. L.; Erikson, R. L.; Simmons, D. L. *Proc. Natl. Acad. Sci. U.S.A.* **1991**, *88*, 2692–2696.
9. Kujubu, D. A.; Fletcher, B. S.; Varnum, B. C.; Lim, R. W.; Herschman, H. R. *J. Biol. Chem.* **1991**, *266*, 12866–12872.
10. Masferrer, J. L.; Seibert, K.; Zweifel, B.; Needleman, P. *Proc. Natl. Acad. Sci. U.S.A.* **1992**, *89*, 3917–3921.
11. For a review, see: Reitz, D. B.; Seibert, K. *Annu. Rep. Med. Chem.* **1995**, *30*, 179–188.
12. For a review, see: Reitz, D. B.; Isakson, P. C. *Curr. Pharm. Des.* **1995**, *1*, 211–220.
13. For a review see: Kalgutkar, A. M.; Zhao, Z. *Curr. Drug Targets* **2001**, *2*, 79–106.
14. Penning, T. D.; Talley, J. J.; Bertenshaw, S. R.; Carter, J. S.; Collins, P. W.; Docter, S.; Graneto, M. J.; Lee, L. F.; Malecha, J. W.; Miyashiro, J. M.; Rogers, R. S.; Rogier, D. J.; Yu, S. S.; Anderson, G. D.; Burton, E. G.; Cogburn, J. N.; Gregory, S. A.; Koboldt, C. M.; Perkins, W. E.; Seibert, K.; Veenhuizen, A. W.; Zhang, Y. Y.; Isakson, P. C. *J. Med. Chem.* **1997**, *40*, 1347–1365.
15. Prasit, P.; Wang, Z.; Brideau, C.; Chan, C.-C.; Charleson, S.; Cromlish, W.; Ethier, D.; Evans, J. F.; Ford-Hutchinson, A. W.; Gauthier, J. Y.; Gordon, R.; Guay, J.; Gresser, M.; Kargman, S.; Kennedy, B.; Leblanc, Y.; Léger, S.; Mancini, J.; O'Neill, G. P.; Ouellet, M.; Percival, M. D.; Perrier, H.; Riendeau, D.; Rodger, Y.; Tagari, P.; Thérien, M.; Vickers, P.; Wong, E.; Xu, L.-J.; Young, R. N.; Zamboni, R. *Bioorg. Med. Chem. Lett.* **1999**, *9*, 1773–1778.
16. Biava, M.; Porretta, G. C.; Cappelli, A.; Vomero, S.; Manetti, F.; Botta, M.; Sautebin, L.; Rossi, A.; Makovec, F.; Anzini, M. *J. Med. Chem.* **2005**, *48*, 3428–3432.
17. Salvadori, P.; Di Bari, L.; Pescitelli, G. In *Circular Dichroism: Principles and Applications*; 2nd ed.; Nakanishi, K., Berova, N., Woody, R. W., Eds., HPLC–CD: Stereochemical Analysis at Work; Wiley-VCH: New York, 2000; pp 797–817.
18. For some recent examples, see: (a) Di Bari, L.; Guillarme, S.; Hermitage, S.; Jay, D. A.; Pescitelli, G.; Whiting, A. *Chirality* **2005**, *17*, 323–331; (b) Cappelli, C.; Bronco, S.; Monti, S. *Chirality* **2005**, *17*, 577–589; (c) Seibert, S. F.; König, G. M.; Voloshina, E.; Raabe, G.; Fleischhauer, J. *Chirality* **2006**, *18*, 413–418; (d) McCann, D. M.; Stephens, P. J. *J. Org. Chem.* **2006**, *71*, 6074–6098; (e) Stephens, P. J.; McCann, D. M.; Devlin, F. J.; Smith, A. B. *J. Nat. Prod.* **2006**, *69*, 1055–1064; (f) Hussain, H.; Krohn, K.; Floerke, U.; Schulz, B.; Draeger,

S.; Pescitelli, G.; Antus, S.; Kurtán, T. *Eur. J. Org. Chem.* **2007**, 292–295.
19. Cramer, C. J. *Essentials of Computational Chemistry: Theories and Models*, 2nd ed.; Wiley: Chichester, 2004; p 501ff.
20. Berova, N.; Nakanishi, K. In *Circular Dichroism: Principles and Applications*; 2nd ed.; Nakanishi, K., Berova, N., Woody, R. W., Eds., Wiley-VCH: New York, 2000; Chapter 12, pp 337–382.
21. (a) Wiesler, W. T.; Nakanishi, K. *J. Am. Chem. Soc.* **1990**, *112*, 5574–5583; (b) Zhou, P.; Zhao, N.; Rele, D. N.; Berova, N.; Nakanishi, K. *J. Am. Chem. Soc.* **1993**, *115*, 9313–9314; (c) Nehira, T.; Parish, C. A.; Jockusch, S.; Turro, N. J.; Nakanishi, K.; Berova, N. *J. Am. Chem. Soc.* **1999**, *121*, 8681–8691; (d) Tanaka, K.; Pescitelli, G.; Nakanishi, K.; Berova, N. *Monatsh. Chem.-Chem. Mon.* **2005**, *136*, 367–395.
22. (a) Baxter, N. J.; Williamson, M. P. *J. Biomol. NMR* **1997**, *9*, 359–369; (b) Cierpicki, T.; Otlewski, J. *J. Biomol. NMR* **2001**, *21*, 249–261.
23. Kamlet, M. J.; Abboud, J.-L. M.; Abraham, M. H.; Taft, R. W. *J. Org. Chem.* **1983**, *48*, 2877–2887.
24. (a) Silverstein, R. M.; Webster, F. X.; Kiemle, D. *Spectrometric Identification of Organic Compounds*, 7th ed.; Wiley: New York, 2005, pp 95–98; (b) Mori, N.; Asano, Y.; Tsuzuki, Y. *Bull. Chem. Soc. Jpn.* **1968**, *41*, 1871–1875.
25. See for example: (a) Furse, K. E.; Pratt, D. A.; Porter, N. A.; Lybrand, T. P. *Biochemistry* **2006**, *45*, 3189–3205; (b) Singh, P.; Kaur, P.; Mittal, A.; Kumar, S. *Indian J. Chem. B* **2006**, *45B*, 1692–1698; (c) Park, H.; Lee, S. *J. Comput. Aided Mol. Des.* **2005**, *19*, 17–31; (d) Perez-Maseda, C.; Calvet, C.; Cuberes, R.; Frigola, J. *Electrophoresis* **2003**, *24*, 1416–1421; (e) Handley, D. A.; Cervoni, P.; McCray, J. E.; McCullough, J. R. *J. Clin. Pharmacol.* **1998**, *38*, 25S–35S; (f) Furse, K. E.; Pratt, D. A.; Porter, N. A.; Lybrand, T. P. *Biochemistry* **2006**, *45*, 3189–3205.
26. Frisch, M. J.; Trucks, G. W.; Schlegel, H. B.; Scuseria, G. E.; Robb, M. A.; Cheeseman, J. R.; Montgomery, J. A., Jr.; Vreven, T.; Kudin, K. N.; Burant, J. C.; Millam, J. M.; Iyengar, S. S.; Tomasi, J.; Barone, V.; Mennucci, B.; Cossi, M.; Scalmani, G.; Rega, N.; Petersson, G. A.; Nakatsuji, H.; Hada, M.; Ehara, M.; Toyota, K.; Fukuda, R.; Hasegawa, J.; Ishida, M.; Nakajima, T.; Honda, Y.; Kitao, O.; Nakai, H.; Klene, M.; Li, X.; Knox, J. E.; Hratchian, H. P.; Cross, J. B.; Adamo, C.; Jaramillo, J.; Gomperts, R.; Stratmann, R. E.; Yazyev, O.; Austin, A. J.; Cammi, R.; Pomelli, C.; Ochterski, J. W.; Ayala, P. Y.; Morokuma, K.; Voth, G. A.; Salvador, P.; Dannenberg, J. J.; Zakrzewski, V. G.; Dapprich, S.; Daniels, A. D.; Strain, M. C.; Farkas, O.; Malick, D. K.; Rabuck, A. D.; Raghavachari, K.; Foresman, J. B.; Ortiz, J. V.; Cui, Q.; Baboul, A. G.; Clifford, S.; Cioslowski, J.; Stefanov, B. B.; Liu, G.; Liashenko, A.; Piskorz, P.; Komaromi, I.; Martin, R. L.; Fox, D. J.; Keith, T.; Al-Laham, M. A.; Peng, C. Y.; Nanayakkara, A.; Challacombe, M.; Gill, P. M. W.; Johnson, B.; Chen, W.; Wong, M. W.; Gonzalez, C.; Pople, J. A. *Gaussian 03, Revision B.05*; Gaussian: Pittsburgh PA, 2003.
27. See Gaussian'03 documentation at http://www.gaussian.com/g_ur/g03mantop.htm for reference on calculation methods, basis sets and density functionals.